Journal of Crystal Growth 518 (2019) 1–4

Contents lists available at ScienceDirect

Journal of Crystal Growth

journal homepage: www.elsevier.com/locate/jcrysgro

# Comparing the magnetic and magnetoelectric properties of the $SmFe_3(BO_3)_4$ ferroborate single crystals grown using different solvents

Evgeniy Eremin[a,b,c,*], Irina Gudim[a], Vladislav Temerov[a], Dmitriy Smolyakov[a], Maxim Molokeev[a,b]

[a] Kirensky Institute of Physics, Federal Research Center KSC SB RAS, Krasnoyarsk 660036, Russia
[b] Siberian Federal University, Krasnoyarsk 660041, Russia
[c] Siberian State University of Science and Technologies, Krasnoyarsk 660037, Russia

ARTICLE INFO

Communicated by V. Fratello

*Keywords:*
A.1. Impurities
A.2. Growth from solutions
A.2. Single crystal growth
B.1. Borates
B.2. Ferroelectric materials
B.2. Magnetic materials

ABSTRACT

$SmFe_3(BO_3)_4$ single crystals have been grown from the bismuth trimolybdate and lithium tungstate-based melt–solutions. Samarium ferroborate single crystals were grown first from the lithium–tungstate flux. The magnetic and magnetoelectric properties of the synthesized crystals have been compared. It is shown that the $SmFe_3(BO_3)_4$ ferroborate grown from the bismuth trimolybdate-based melt–solution contains impurities of $Bi^{3+}$ ions (~5% at.), which replace $Sm^{3+}$ ions, while the $SmFe_3(BO_3)_4$, ferroborate grown from the lithium tungstate-based melt–solution contains minor or zero amounts of such impurities. The magnetoelectric and magnetodielectric effects with the $Bi^{3+}$ admixture appeared 1.5× stronger than in $SmFe_3(BO_3)_4$; this is probably due to twinning.

## 1. Introduction

In recent years, $RFe_3(BO_3)_4$ (R = Y, La-Lu) rare-earth ferroborates with a huntite structure have been in focus of researchers due to their multiferroic properties [1,2]. The main element of the rare-earth ferroborate crystal structure (sp. gr. *R32* at high temperatures) is spiral chains of edge-sharing $FeO_6$ octahedra oriented along the *c* (third-order) axis. In the crystal structure of these compounds, the exchange coupling inside a chain is much stronger than the interchain coupling.

Magnetically, ferroborates are antiferromagnets with two (rare-earth and iron) interacting magnetic subsystems. The iron subsystem is ordered at $T_N$ = 30–40 K. The rare-earth subsystem is magnetized by the *f-d* interaction and essentially contributes to the magnetic anisotropy and orientation of the magnetic moment.

The first technique developed for growing isostructural nonlinear-optical trigonal $RAl_3(BO_3)_4$ aluminoborate crystals was based on using $K_2Mo_3O_{10}$–$B_2O_3$ potassium trimolybdate melt–solutions [3]. Then, it was proposed to synthesize the $RAl_3(BO_3)_4$ and $RFe_3(BO_3)_4$ single crystals using $Bi_2Mo_3O_{12}$–$B_2O_3$ bismuth trimolybdate melt–solutions [4], in which $Bi_2O_3$ and $MoO_3$ are coupled stronger than $K_2O_3$ and $MoO_3$. Therefore, the substitution of bismuth and molybdenum in the grown crystal for the rare-earth element was assumed to be relatively weak [5]. However, as was shown by the chemical and structural studies for the $GdFe_3(BO_3)_4$ ferroborate [6], $Bi^{3+}$ ions replace the rare-earth ion in an amount up to 5 at.%, which is smaller as compared with substitution of potassium and molybdenum [5]. At that time, the lithium tungstate-based melt–solutions were proposed.

It is well-known that the oxide compounds containing $Bi^{3+}$ or $Pb^{2+}$ ions have an unbound (lone) electron pair on the *s* orbital and can establish the conditions for the occurrence of local dipoles in the crystal structure, which inevitably affects the electrical properties of a compound [7] and, in addition, can influence the magnetoelectric properties.

The aim of this study was to investigate the effect of the $Bi^{3+}$ ion impurity on the magnetic and magnetoelectric properties of rare-earth ferroborates with the huntite structure. A technique for growing $SmFe_3(BO_3)_4$ single crystals from a new $Li_2WO_4$–$B_2O_3$ lithium tungstate melt-solution was developed. The particular interest in the $SmFe_3(BO_3)_4$ compound is due to its magnetoelectric effect [8] greatest among all single-component ferroborates and the giant magnetodielectric effect [9].

In this work, we compare the magnetic and magnetoelectric properties of the $SmFe_3(BO_3)_4$ single crystals grown using a new $Li_2WO_4$–$B_2O_3$ solvent and the $SmFe_3(BO_3)_4$ compound grown using the previously developed bismuth trimolybdate solvent in order to establish the effect of the $Bi^{3+}$ impurity on the magnetic and magnetoelectric

* Corresponding author at: Kirensky Institute of Physics, Federal Research Center KSC SB RAS, Krasnoyarsk 660036, Russia.
*E-mail address:* eev@iph.krasn.ru (E. Eremin).

https://doi.org/10.1016/j.jcrysgro.2019.04.017
Received 2 October 2018; Received in revised form 17 April 2019; Accepted 18 April 2019
Available online 19 April 2019

properties of $SmFe_3(BO_3)_4$.

## 2. Growing the single crystals

The $SmFe_3(BO_3)_4$ single crystals were grown from the bismuth trimolybdate and lithium tungstate melt–solutions [10,11].

### 2.1. Phase formation

First, let us discuss the control of nucleation of the $SmFe_3(BO_3)_4$ crystal trigonal phases for the two melt–solution systems: $Bi_2Mo_3O_{12}$–$B_2O_3$–$Sm_2O_3$–$Fe_2O_3$ and $Li_2WO_4$–$B_2O_3$–$Sm_2O_3$–$Fe_2O_3$.

The investigated melt–solution systems can be expressed in the quasi-binary form:

$$78\%\ \text{mass.}\,[Bi_2Mo_3O_{12} + 3{,}2B_2O_3 + 0{,}5Sm_2O_3] + 22\%\ \text{mass.}\,SmFe_3(BO_3)_4 \quad (1)$$

$$75\%\ \text{mass.}\,[Li_2WO_4 + 3{,}6B_2O_3 + 0{,}3Sm_2O_3] + 25\%\ \text{mass.}\,SmFe_3(BO_3)_4 \quad (2)$$

The 150-g melt-solution weights were prepared at T = 1000–1100 °C by sequential melting of the corresponding oxides [$Bi_2O_3$ (reagent grade) and $MoO_3$ (analytical grade) or $Li_2WO_4$ (analytical grade)], $B_2O_3$ (special-purity grade), [$Fe_2O_3$ (special-purity grade), $Sm_2O_3$ (SmO-L)](domestic reagents) in a platinum cylindrical crucible with a 50 mm diameter and 60 mm height. Then, the crucible with the melt–solution was placed in a furnace with a temperature gradient, the vertical component of which at $T$ = 1000 °C decreases at a rate of 2–3 °C/cm from the bottom to the top of the crucible. After melt–solution homogenization at $T$ = 1000 °C for 24 h, the temperature was reduced to the expected saturation temperature ($T_{sat}$) and a platinum wire crystal carrier 4 mm in diameter was immersed into the melt–solution. After 1–2 h, the crystal carrier was withdrawn and the nucleation on it was estimated. Then, the probes were continued with the temperature decreasing down to $T \approx 850$ °C with a step of 10–20 °C without intermediate overheat of solution. Thereafter the saturation temperature was determined with an accuracy of ± 2 °C using test crystals. For the first melt solution, the saturation temperature was 965 °C and for the second 973 °C.

It was established previously that hematite α-$Fe_2O_3$ is in the single crystallizing phase without an excess of $B_2O_3$ and $Sm_2O_3$ in the melt in the temperature range from its $T_{sat}$ to 850 °C. As the $B_2O_3$ and $Sm_2O_3$ contents increase to 3 and 0.4 mol respectively, hematite remains in the high-temperature phase and $Fe_3BO_6$ crystallites arise in the lower part of the temperature interval. The α-$Fe_2O_3$ and $Fe_3BO_6$ phases continue forming, but they occur closer to the lower $SmFe_3(BO_3)_4$ metastability zone boundary and, at a certain time after the formation, start dissolving (the nonequilibrium effect) [10]. The lower boundary of the $SmFe_3(BO_3)_4$ metastability zone is the maximum supercooling, where spontaneous crystals do not form on the superheated rod for 24 h.

The nonequilibrium effect and its relaxation time were estimated by observing simultaneously the behavior of the equilibrium and labile phases immersed in the flux. At a temperature of 12 °C below the $SmFe_3(BO_3)_4$ formation, noticeable α-$Fe_2O_3$ and $Fe_3BO_6$ dissolution was observed at 10–16 h; with an increase in supercooling to 20 °C, this period was over 1 day. The overcooling threshold, after which any labile phase nucleated, significantly depends on $B_2O_3$ and $Sm_2O_3$ content. This additionally narrows the range of their possible content values and requires preventing their significant deviation during the flux preparation because of the uncontrollable variation in the composition due to evaporation. Trigonal $SmFe_3(BO_3)_4$ becomes the sole high-temperature phase with a wide stability range only at $3{,}2B_2O_3$ and $0{,}3Sm_2O_3$ for first system and $3{,}6B_2O_3$ and $0{,}6Sm_2O_3$ for second one at temperatures up to 850 °C. Grown single crystals have a typical huntite crystal shape (Fig. 1) [3].

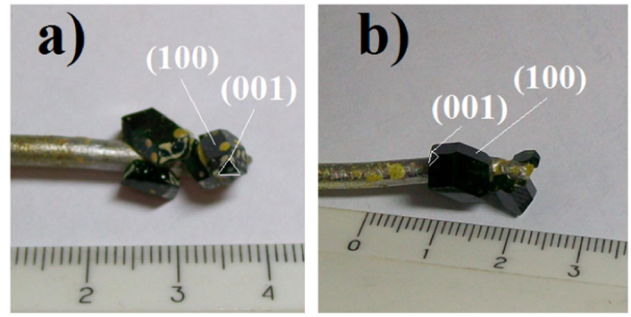


**Fig. 1.** $SmFe_3(BO_3)_4$ single crystals grown in fluxes based on (a) bismuth trimolybdate, (b) lithium tungstate.

### 2.2. Preparing seeds

Since the number of the crystals grown by spontaneous nucleation is unknown, we cannot set an optimal rate of temperature reduction. The crystals growth from seeds is easier to control.

At $T$ = 1000 °C, the wire crystal carrier was immersed into the flux and reversal rotated at 30 rpm. The furnace temperature was decreased to $T = T_{sat} - 12$ °C. After 2 h, the crystal carrier was withdrawn from the furnace. Thus, few crystallites were formed of a cooled flux enveloping carrier of crystals. After that, the crystal carrier was immersed into the flux again (without overheating at the same temperature $T = T_{sat} - 12$ °C) and rotated at 30 rpm with a change of direction every minute. In the next 24 h, 10–30 crystals 0.5–2 mm in size grew. They were high-quality and were used as seeds.

### 2.3. Seed growth of the crystals

Without knowing the number of crystals, we cannot calculate the temperature decrease rate that would ensure a crystal growth rate of no more than 0.5 mm per day. The growing crystal inherits all seed defects, so we use small seeds. The seeds were placed into holder holes.

The crystal carrier with four high-quality seeds smaller than 1 mm in size was suspended above the flux at $T$ = 1000 °C. After that, the temperature was decreased to $T = T_{sat} + 7$ °C and the crystal holder with seeds was immersed into the flux to a depth of 25–30 mm and the rotation with a speed of 30 rpm and a reversal period of 1 min was switched on. After 15 min, the temperature was decreased to $T = T_{sat} - 5$ °C. Then, the temperature was decreased by 1–3 °C per day, according to a special program. In 9–13 days, the growth process was finished. The crystal carrier was lifted above the flux and cooled to room temperature with the furnace supply switched-off. The grown crystals were about 6–10 mm in size, which is sufficient for studying their physical properties. No spontaneous formation and foreign phases were observed.

## 3. The magnetic and magnetoelectric properties

The magnetic study was carried out on a Physical Property Measurement System (Quantum Design) in the temperature range of 4.2–300 K and a magnetic field of 1 kOe. To measure the magnetoelectric polarization and permittivity on the face of the sample in the form of a plane-parallel plate (the faces were perpendicular to the *a* axis), epoxy resin electrodes with a conductive filler were formed. The charge induced in the sample by the magnetoelectric effect was measured with a Keithley 6517B electrometer. The dielectric properties were measured with an E4980A Precision Agilent LCR-meter at a frequency of 100 kHz.

As was shown in [6], the use of the bismuth trimolybdate solvent leads to the occurrence of the $Bi^{3+}$ ion impurity in the crystal; therefore, the crystals grown from this melt–solution are hereinafter referred to as $SmFe_3(BO_3)_4$:Bi and the crystals grown from the lithium tungstate

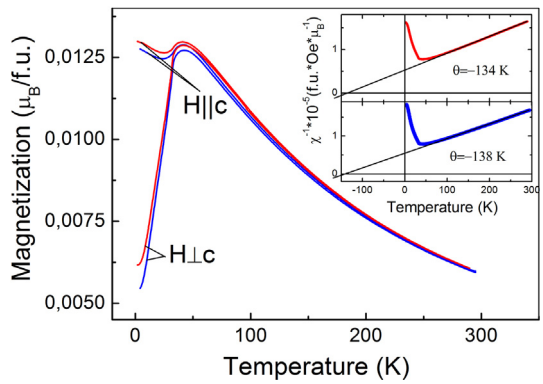


**Fig. 2.** Thermal dependencies of magnetization of $SmFe_3(BO_3)_4$ (blue) and $SmFe_3(BO_3)_4$:Bi (red) oxyborate with huntite structure measured in a magnetic field of 1 kOe directed along the crystallographic *c* axis (H||c) and in the basal plane along the *a* axis (H⊥c). Inset shows temperature dependence of the reciprocal magnetic susceptibility $\chi^{-1}$.

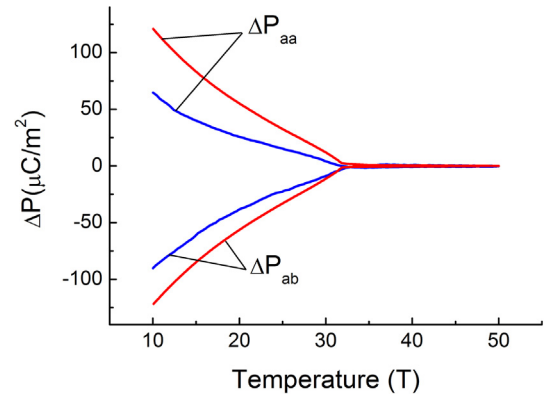


**Fig. 3.** Thermal dependencies of the magnetoelectric polarization of the $SmFe_3(BO_3)_4$ (blue) and $SmFe_3(BO_3)_4$:Bi (red) oxyborate with huntite structure measured in a magnetic field of 50 kOe directed along the crystallographic *a* axis ($\Delta P_{aa}$) and along the *b* axis, which is perpendicular to the *a* and *c* axes ($\Delta P_{ab}$). (For interpretation of the references to colour in this figure legend, the reader is referred to the web version of this article.)

melt–solution, as $SmFe_3(BO_3)_4$, since, in this case, uncontrolled impurities of $Bi^{3+}$ are not expected.

Fig. 2 shows the temperature dependences of magnetization for the $SmFe_3(BO_3)_4$ single crystals grown using different solvents (bismuth trimolybdate and lithium tungstate). The temperature dependence of magnetizations $M_{||}$ and $M_{\perp}$ was measured in a magnetic field of 1 kOe directed along the crystallographic *c* axis and in the basal plane along the *a* axis, respectively.

At temperatures of $T < T_N \approx 32$ K, the magnetization behavior for both crystals is not qualitatively different from the behavior observed earlier in $SmFe_3(BO_3)_4$ [12,13]. The magnetization in the basal plane decreases monotonically with a decrease in temperature; along the *c* axis, its value equal to the value at the Neel point remains almost invariable. This is indicative of the fact that the magnetic moments of $Fe^{3+}$ ions are ordered in the basal plane.

In the paramagnetic region, the magnetization of both compositions is isotropic and obeys the Curie–Weiss law (inset to Fig. 2). The experimental paramagnetic Curie temperatures differ insignificantly and amount to $\theta_1 = -138$ K for $SmFe_3(BO_3)_4$ and $\theta_2 = -134$ K for $SmFe_3(BO_3)_4$:Bi. The negative sign is indicative of the antiferromagnetic exchange coupling in the magnetic system. It can be seen that the paramagnetic Curie temperature of $SmFe_3(BO_3)_4$:Bi is lower. It decreases, as expected, upon substitution of nonmagnetic bismuth $Bi^{3+}$ ions for magnetic $Sm^{3+}$ ions. Substitution also decreases the effective magnetic moment experimentally determined by the Curie–Weiss law $\mu_{eff} = 10.71\ \mu_B$ for $SmFe_3(BO_3)_4$ and $\mu_{eff} = 10.7\ \mu_B$ for $SmFe_3(BO_3)_4$:Bi. At the same time, the magnetization of the compound increases (Fig. 2). This behavior was explained in the framework of a simple phenomenological model by the example of $Sm_{1-x}La_xFe_3(BO_3)_4$ solid solutions [14], in which the magnetic moment increases and paramagnetic Curie temperature decreases upon substitution of nonmagnetic $La^{3+}$ ions for magnetic $Sm^{3+}$ ions.

Thus, the magnetic investigations showed that in the $SmFe_3(BO_3)_4$ ferroborate crystals grown using the bismuth trimolybdate melt–solution, $Bi^{3+}$ ions replace $Sm^{3+}$ ions.

Fig. 3 presents temperature dependences of the magnetoelectric polarization of the $SmFe_3(BO_3)_4$ and $SmFe_3(BO_3)_4$:Bi single crystals in a field of 50 kOe. The magnetic field was applied along with the second-order crystallographic *a* axis and along the *b* axis, which is perpendicular to the *a* and *c* axes. It can be seen that the magnetoelectric response in $SmFe_3(BO_3)_4$:Bi is higher than in $SmFe_3(BO_3)_4$ by a factor of about 1.5.

At first it was assumed that the above result could be related to the effect of the $Bi^{3+}$ admixture on the magnetoelectric properties. However, as we already know, in trigonal ferroborates with the huntite structure, domains with the right and left spirals (twinning), consisting of oxygen octahedra with $Fe^{3+}$ ions, can coexist along the third-order axis [14]. As was shown in [15], the twinning decreases the magnetoelectric polarization. In this case, the polarization is determined as a difference between the contributions of the right and left isomers subsystem.

In addition, the difference between the magnetoelectric polarization values can be caused by the change in the crystal field due to local distortions of the anionic environment of the rare-earth ion resulting from the presence of the $Bi^{3+}$ impurity. This seems quite reasonable, since, for example, the difference between the values of the magnetoelectric effect in $HoAl_3(BO_3)_4$ [16] and $HoGa_3(BO_3)_4$ [17] was attributed to the effect of different crystal fields of these two oxyborates, which form the $Ho^{3+}$ ion electronic structure.

The temperature dependences of the permittivity in a magnetic field of 8 kOe and without it for the two samples are presented in Fig. 4. The inset Fig. 4 shows that the value of magnetodielectric effect (MDE = ([$\varepsilon(H) - \varepsilon(0)/\varepsilon(0)$] * 100%)) in $SmFe_3(BO_3)_4$:Bi is higher than in $SmFe_3(BO_3)_4$ by a factor of 1.5, which is similar to the ratio between the magnetoelectric effects in these compounds. Since the magnetodielectric effect is governed by the same mechanisms as the magnetoelectric effect, this result is quite expected. However, the surprising result was the greater increase in the permittivity below the Néel temperature for $SmFe_3(BO_3)_4$ ($\varepsilon(T = 5\text{ K})/\varepsilon(T = 40\text{ K}) = 1.5$) as

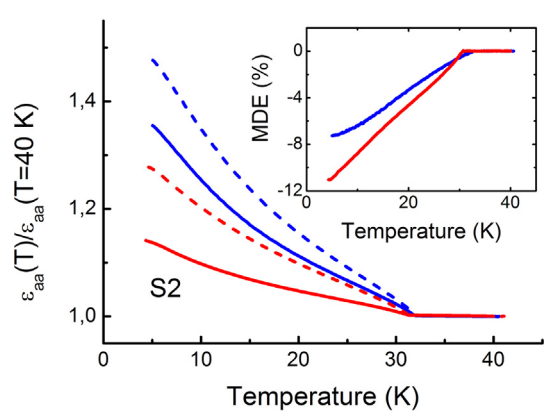


**Fig. 4.** Thermal dependencies of the permittivity of the $SmFe_3(BO_3)_4$ (blue) and $SmFe_3(BO_3)_4$:Bi (red) oxyborate with huntite structure measured in a magnetic field H = 8 kOe (solid) and H = 0 (dash). The inset shows thermal dependencies of the magnetodielectric effect MDE = ([$\varepsilon$(8 kOe) − $\varepsilon$(0)/$\varepsilon$(0)] * 100%). (For interpretation of the references to colour in this figure legend, the reader is referred to the web version of this article.)

compared with $SmFe_3(BO_3)_4$:Bi ($\varepsilon$(T = 5 K)/$\varepsilon$(T = 40 K) = 1.3) (Fig. 4).

To test the effect of twinning on the magnitude of the magnetoelectric effect, we determined the ratio of the left and right isomers in each sample. The study was carried out with a SMART APEX II diffractometer (Mo Ka, λ = 0.7106 Å) at room temperature. Each crystal was broken and four microcrystals from different areas of each crystal were taken for research. It was determined that $SmFe_3(BO_3)_4$:Bi has an average ratio of left and right isomers of 0/100 and $SmFe_3(BO_3)_4$ has a ratio of 82/18. The relative error in the definition of twinning does not exceed 8%.

It can be seen that the polarization of $SmFe_3(BO_3)_4$ has a smaller value, primarily due to the presence of twinning in this sample. If we assume that there was no twinning, then its polarization would increase by about 100/(82 – 18) ≈ 1.5 times. Thus, we have to admit that the difference in the magnetoelectric effect of the studied crystals is mainly determined by the factor of twinning. Study of the influence of bismuth ions impurity on the magnetoelectric properties of rare-earth huntite requires further research.

## 4. Conclusions

The $SmFe_3(BO_3)_4$ single crystals were grown first from the lithium tungstate-based melt–solution. For comparison, the $SmFe_3(BO_3)_4$ single crystals were grown using the bismuth trimolybdate solvent. The magnetic and magnetoelectric properties of the synthesized ferroborates were compared.

According to the results of the magnetic study, the use of the bismuth trimolybdate solvent leads to the substitution of small (about 5 at. %) amounts of $Bi^{3+}$ ions for $Sm^{3+}$ ions. The use of the lithium tungstate-based solvent makes it possible to grow the $SmFe_3(BO_3)_4$ ferroborate with higher purity.

The magnetoelectric investigations showed that the magnetoelectric effects of the $SmFe_3(BO_3)_4$:$Bi^{3+}$ single crystal are stronger than in the pure (without the $Bi^{3+}$ admixture) samarium ferroborate by a factor of approximately 1.5. This fact was mainly attributed to the influence of twinning in the investigated single crystals.

## Acknowledgement

This study was supported by the Russian Foundation for Basic Research (RFBR) according to the research projects No. 18-02-00696_a and RFBR, Government of Krasnoyarsk Territory, Krasnoyarsk Region Science and Technology Support Fund by project No. 18-42-240011 p_a.

## References

[1] Y. Hinatsu, Y. Doi, K. Ito, M. Wakeshima, A. Alemi, Magnetic and calorimetric studies on rare-earth iron borates $LnFe_3(BO_3)_4$ (Ln = Y, La-Nd, Sm-Ho), J. Solid State Chem. 172 (2003) 438–445, https://doi.org/10.1016/S0022-4596(03)00028-8.

[2] A.K. Zvezdin, S.S. Krotov, A.M. Kadomtseva, G.P. Vorob'ev, YuF. Popov, A.P. Pyatakov, L.N. Bezmaternykh, E.A. Popova, Magnetoelectric effects in gadolinium iron borate $GdFe_3(BO_3)_4$, JETP Lett. 81 (2005) 272–276, https://doi.org/10.1134/1.1931014.

[3] N.I. Leonyuk, L.I. Leonyuk, Growth and characterization of $RM_3(BO_3)_4$ crystals, Progr. Cryst. Growth Charact. 31 (1995) 179–278, https://doi.org/10.1016/0960-8974(96)83730-2.

[4] L.N. Bezmaternykh, V.L. Temerov, I.A. Gudim, N.A. Stolbovaya, Crystallization of trigonal (Tb, Er)(Fe, $G_a)_3(BO_3)_4$ phases with Hantite structure in Bismute trimolybdate-based fluxes, Crystallogr. Rep. 50 (2005) 97–99, https://doi.org/10.1134/1.2133981.

[5] K.N. Boldyrev, M.N. Popova, M. Bettinelli, V.L. Temerov, I.A. Gudim, L.N. Bezmaternykh, P. Loiseau, G. Aka, N.I. Leonyuk, Quality of the rare earth aluminum borate crystals for laser applications, probed by high-resolution spectroscopy of the $Yb^{3+}$ ion, Optic. Mater. 34 (2012) 18851889, https://doi.org/10.1016/j.optmat.2012.05.021.

[6] E.S. Smirnova, O.A. Alekseeva, A.P. Dudka, I.A. Verin, V.V. Artemov, L.N. Bezmaternykh, I.A. Gudim, K.V. Frolov, I.S. Lyubutin, Structure of $Gd_{0.95}Bi_{0.05}Fe_3(BO_3)_4$ single crystals at 293 and 90 K, Crystallogr. Rep. 61 (2016) 558–565, https://doi.org/10.1134/S1063774516040192.

[7] R. Seshadri, G. Baldinozzi, C. Felser, W. Tremel, Visualizing electronic structure changes across an antiferroelectric phase transition: $Pb_2MgWO_6$, J. Mater. Chem. 9 (1999) 2463–2466, https://doi.org/10.1039/a904408f.

[8] Yu.F. Popov, A.P. Pyatakov, A.M. Kadomtseva, G.P. Vorob'ev, A.K. Zvezdin, A.A. Mukhin, V.Yu. Ivanov, I.A. Gudim, Peculiarities in the magnetic, magnetoelectric, and magnetoelastic properties of $SmFe_3(BO_3)_4$ multiferroic, JETP 111 (2010) 199–203, https://doi.org/10.1134/S1063776110080066.

[9] A.A. Mukhin, G.P. Vorob'ev, V.Yu. Ivanov, A.M. Kadomtseva, A.S. Narizhnaya, A.M. Kuz'menko, YuF. Popov, L.N. Bezmaternykh, I.A. Gudim, Colossal magnetodielectric effect in $SmFe_3(BO_3)_4$ multiferroic, JETP Lett. 93 (2011) 275–281, https://doi.org/10.1134/S0021364011050079.

[10] L.N. Bezmaternykh, S.A. Kharlamova, V.L. Temerov, Flux crystallization of trigonal $GdFe_3(BO_3)_4$ competing with the crystallization of α-$Fe_2O_3$, Crist Rep. (2004) 855–857, https://doi.org/10.1134/1.1803319.

[11] M.N. Popova, B.Z. Malkin, K.N. Boldyrev, T.N. Stanislavchuk, D.A. Erofeev, V.L. Temerov, I.A. Gudim, Evidence for a collinear easy-plane magnetic structure of multiferroic $EuFe_3(BO_3)_4$: spectroscopic and theoretical studies, Phys. Rev. B 94 (2016) 184418, https://doi.org/10.1103/PhysRevB.94.184418.

[12] A.A. Demidov, D.V. Volkov, I.A. Gudim, E.V. Eremein, V.L. Temerov, Magnetic properties of the rare-earth ferroborate $SmFe_3(BO_3)_4$, JETP 116 (2013) 800–805, https://doi.org/10.1134/S1063776113050038.

[13] E.V. Eremin, N.V. Volkov, V.L. Temerov, I.A. Gudim, A.F. Bovina, Specific features of magnetic properties of rare-earth ferroborates $Sm_{1-x}La_xFe_3(BO_3)_4$, Phys. Solid State 57 (2015) 569–575, https://doi.org/10.1134/S1063783415030051.

[14] T. Usui, Y. Tanaka, H. Nakajima, M. Taguchi, A. Chainani, M. Oura, S. Shin, N. Katayama, H. Sawa, Y. Wakabayashi, T. Kimura, Observation of quadrupole helix chirality and its domain structure in $DyFe_3(BO_3)_4$, Nat. Mater. 13 (2014) 611–618, https://doi.org/10.1038/NMAT3942.

[15] I.A. Gudim, E.V. Eremin, M.S. Molokeev, V.L. Temerov, N.V. Volkov, Magnetoelectric polarization of paramagnetic $HoAl_{3-x}Ga_X(BO_3)(_4)$ single crystals, trend in magnetism, Nanomagnetism 215 (2014) 364–367, https://doi.org/10.4028/www.scientific.net/SSP.215.364.

[16] A.I. Begunov, A.A. Demidov, I.A. Gudim, E.V. Eremin, Features of the magnetic and magnetoelectric properties of $HoAl_3(BO_3)_4$, JETP Lett. 97 (2013) 528–534, https://doi.org/10.1134/S002136401309004X.

[17] N.V. Volkov, I.A. Gudim, E.V. Eremin, A.I. Begunov, A.A. Demidov, K.N. Boldyrev, Magnetization, magnetoelectric polarization, and specific heat of $HoGa_3(BO_3)_4$, JETP Lett. 99 (2014) 67–75, https://doi.org/10.-1134/S0021364014020106.